Karlsruher Institut für Technologie

Heart-shaped crack-tip zones

- Effect of the zone length

K.G. Schell, C. Bucharsky, G. Rizzi, T. Fett

KIT SCIENTIFIC WORKING PAPERS 148

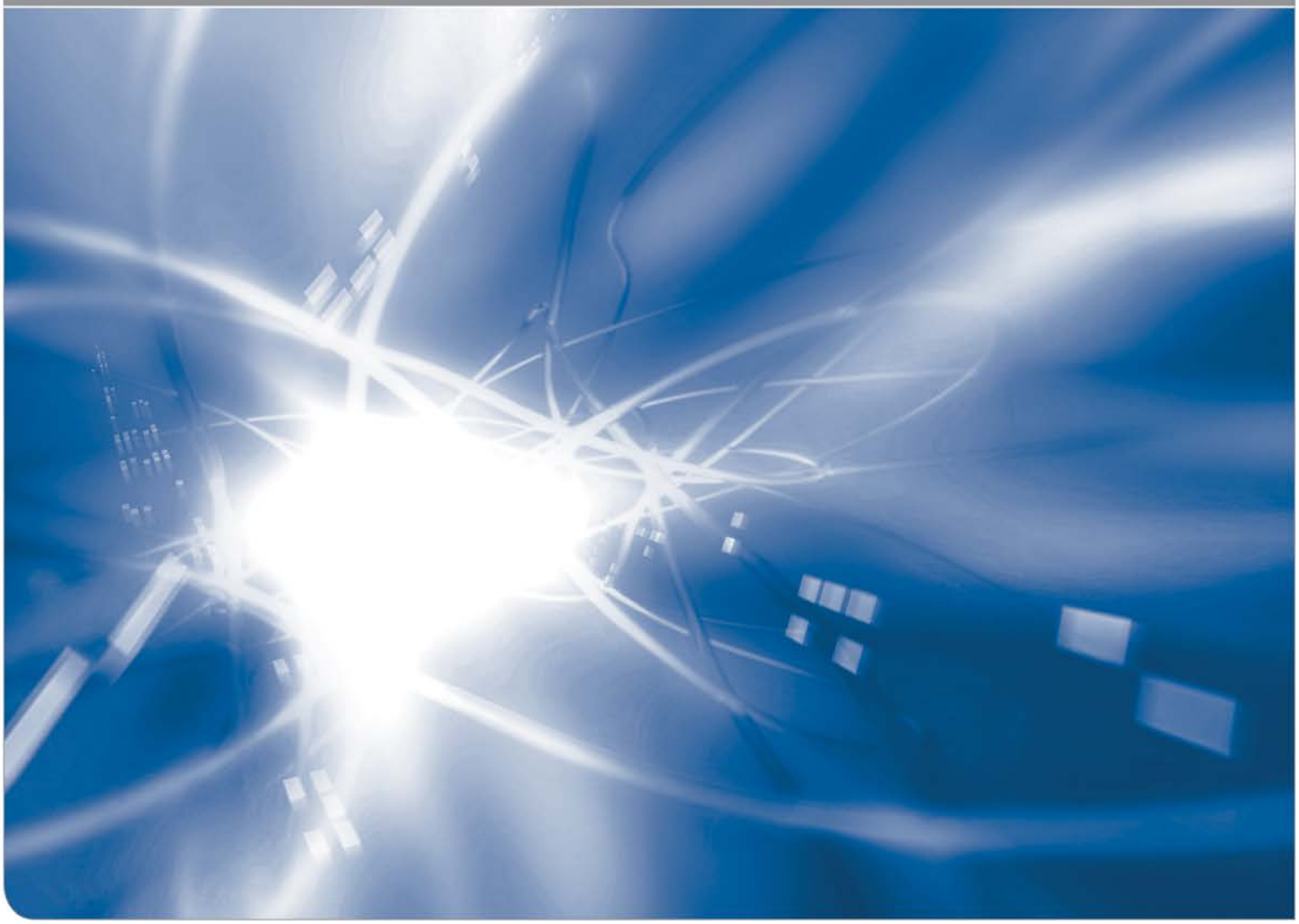

KIT – Universität des Landes Baden-Württemberg und nationales Forschungszentrum in der Helmholtz-Gemeinschaft

IAM Institute for Applied Materials

Impressum

Karlsruher Institut für Technologie (KIT)
www.kit.edu

2020

ISSN: 2194-1629

Abstract

In this report the general influence of different elastic modules ahead of a crack tip and in the bulk on the stress intensity factors will be discussed again.

From the FE results obtained in Report [1], and the theoretical solution by Merkle [3]

$$K = K_{appl}\sqrt{\frac{E}{E_0}}$$

it becomes clear that the FE-results for relative zone sizes $\omega/a > 0$ must deviate from the exact solution but are also in rather good agreement with the theoretic results for finite ω/a.

In this report also results are compiled for cracks fully embedded in zones with reduced module. Such cracks show stress intensity factors completely different from a $\sqrt{E/E_0}$ -dependency.

Nevertheless, it can be concluded that the stress intensity factors on the basis of the J-integral agree with those obtained by COD evaluation.

As an approximate description of the observed E/E_0 dependency we suggest

$$\frac{K}{K_{appl}} \cong \frac{2E}{E + E_0}$$

Contents

1. Introduction

In [1] we compiled stress intensity factor results from a study performed in 2015/2016 for heart-shaped zones ahead of a crack tip showing Young's modules different from the bulk material. We considered the case of constant modulus in the zone, Fig. 1a, and in a single case, the FE-evaluation was made for variable modulus in the zone ahead the tip. As Fig. 1b shows, the modulus was varied in 4 steps. In the inner zone of Fig. 1b, the modulus E was E=0.25 E_0, then E=0.57 E_0, E=0.72 E_0, and outside E=E_0.

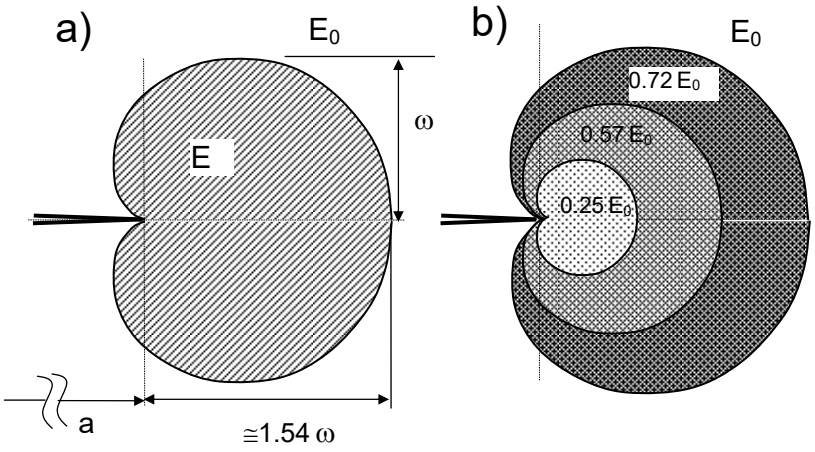

Fig. 1 a) Crack-tip zone with a Young's modulus E deviating from the bulk modulus E_0, E<E_0, b) stepwise decreasing modulus in zones of height 1/3, 2/3, and 3/3ω.

The results from the J-Integral by Rice [2], K_J, obtained in [1] are shown in Fig. 2a (circles and triangle) together with K-values determined from COD in the crack wake and stresses ahead of the tip.

The K-values for the single zones of Fig. 1a are plotted in Fig. 2a by the symbols (for the geometric data see the insert). In this plot all stress intensity factors were normalized on the J-based K value at E/E_0=1, denoted as $K_J(E_0)$. The triangle corresponds to the varying Young's modulus shown in Fig. 1b. Figure 2b represents the ratio of the data for COD- and σ_{yy}-based stress intensity factors normalized on the stress intensity factors from the J-Integral. The hatched area indicates the region of data scatter.

From the results of Fig. 2 we concluded in [1]:

- the stress intensity factors are roughly independent of the computation method,
- the stress intensity factor is only affected by the modulus closest to the crack tip,
- the straight-line in Fig. 2a suggests the representation by

$$K = K_{appl}\sqrt{\frac{E}{E_0}} \tag{1}$$

The FE results confirm eq.(1) as had to be expected e.g. from the theoretical analysis by Merkle [3] on slender notches embedded in the reduced modulus at the notch-root. From the agreement between the theoretical solution by Merkle [3] and the FE-results for $0.1 \le E/E_0 \le 1$, it can be concluded that our crack-zone modelling and the accuracy of our FE-mesh is sufficient at least for this range. For the lowest values of $E/E_0 \le 0.1$, the FE-program indicated deviations.

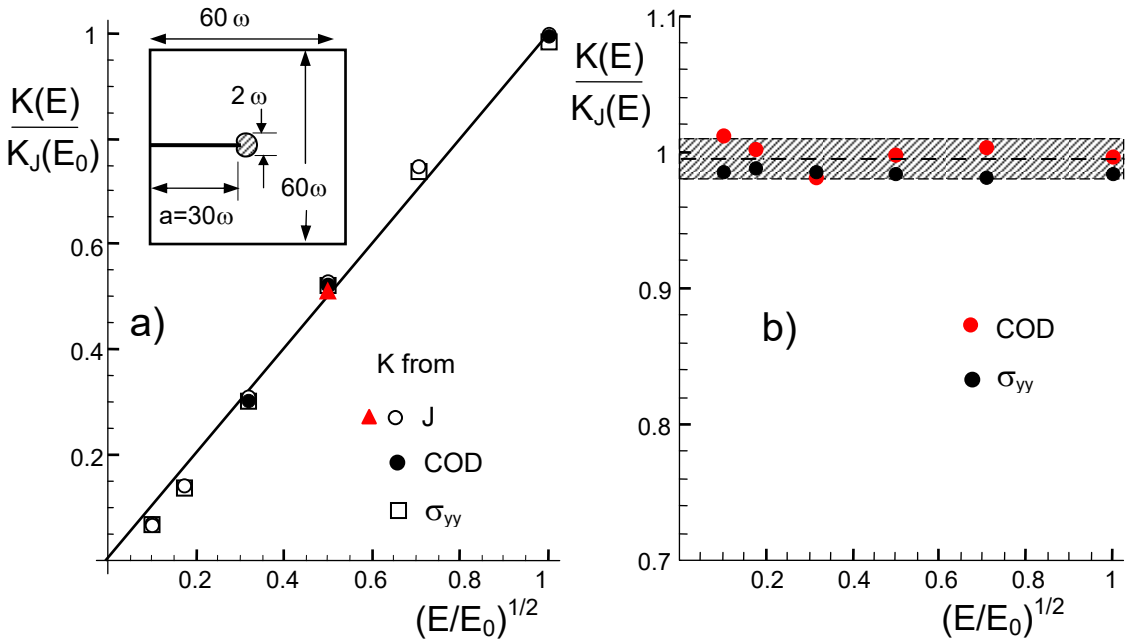

Fig. 2 a) Stress intensity factors from J-Integral, COD, and near-tip stress σ_{yy}, (K-values normalized on the result from J-Integral for $E/E_0=1$), red triangle for step-shaped E-distribution, b) comparison of K from COD and σ_{yy} with the individual results from J-Integral.

For conditions comparable with "small-scale yielding" in elastic-plastic fracture mechanics, i.e. $\omega << (a, W\text{-}a)$, the effect of the zone with reduced E on K_{appl} becomes a "null-effect" [2]. Then it holds

$$K_{appl} = \sigma_0 F(a/W, H/W)\sqrt{\pi a} \qquad (2)$$

with the geometric function F (a/W, H/W) and the remote normal tractions σ_0 at the plate ends.

We used in our study [1] a ratio of $\omega/a=1/30$ and expected that the zone would be sufficiently small to fulfill geometry conditions for small-scale yielding. Despite this relatively small zone, influences from this zone can still be seen in Fig. 2a. This may at least partially be caused by the influence of an effective zone length $a_{eff}=a+\lambda\omega$, $\lambda \ge 0$ with $\lambda=0$ for the case of homogeneous material. In the case of $\lambda>0$, eq.(2) reads

$$K_{appl} = \sigma_0 F(a_{eff}/W, H/W)\sqrt{\pi a_{eff}} \qquad (3)$$

The stress intensity factors for E/E_0=0.25 and ω/a=0, 1/30, and 1/90 are plotted in Fig. 3. A trend with ω/a is visible.

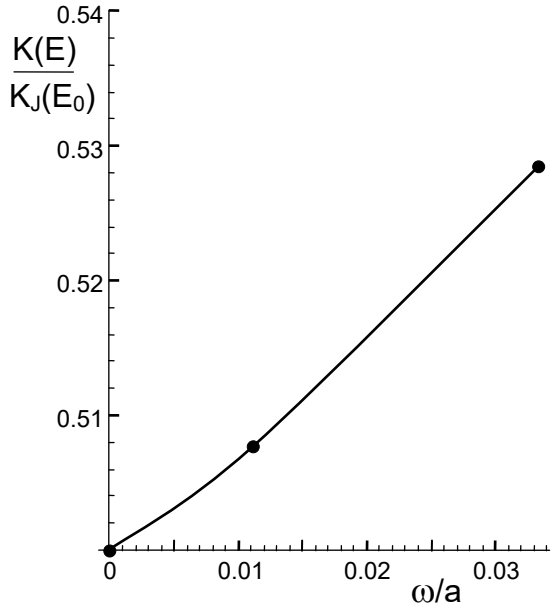

Fig. 3 Stress intensity factor from J-Integral for (E/E_0=0.25).

2. Results for embedded crack tips

While in [1] only zones before the crack tip were considered, in this report we compile results for zones extending additionally over the entire crack length. In this case, the crack tip is fully embedded in the zone with reduced module. The plate dimensions and the crack length were increased by a factor of about 3 in order to reduce any influence of ω/a furthermore. This is shown in the plot of Fig. 4a.

The stress intensity factors exclusively on the basis of the J-Integral are given in Fig. 4a. The squares for $E/E_0 \leq 0.25$ were fitted by

$$\frac{K(E)}{K(E_0)} \cong \frac{2E}{E+E_0} \tag{4}$$

This expression is introduced by the solid curve. The reason for the deviation between the differences for front zone and zones extending in the wake of a crack are actually in discussion and will be addressed in a separate note. Therefore, we only compile our numerical results in this report.

We also evaluated COD-results as done in [1] and obtained the near-tip profiles given in Fig. 5. Stress intensity factors K_{COD} were computed from the Irwin-parabola

$$v = \sqrt{\frac{8}{\pi}} \frac{K_{COD}}{E/(1-\nu^2)} \sqrt{r} \tag{5}$$

where v is the opening displacement and ν Poisson's ratio (0.16 for silica). The displacements in the crack wake are given for the two geometries ω/a=30 and 100. In both cases a/W=a/H=0.5 was kept constant. The plots v vs. $\sqrt{r}$ showed very straight lines.

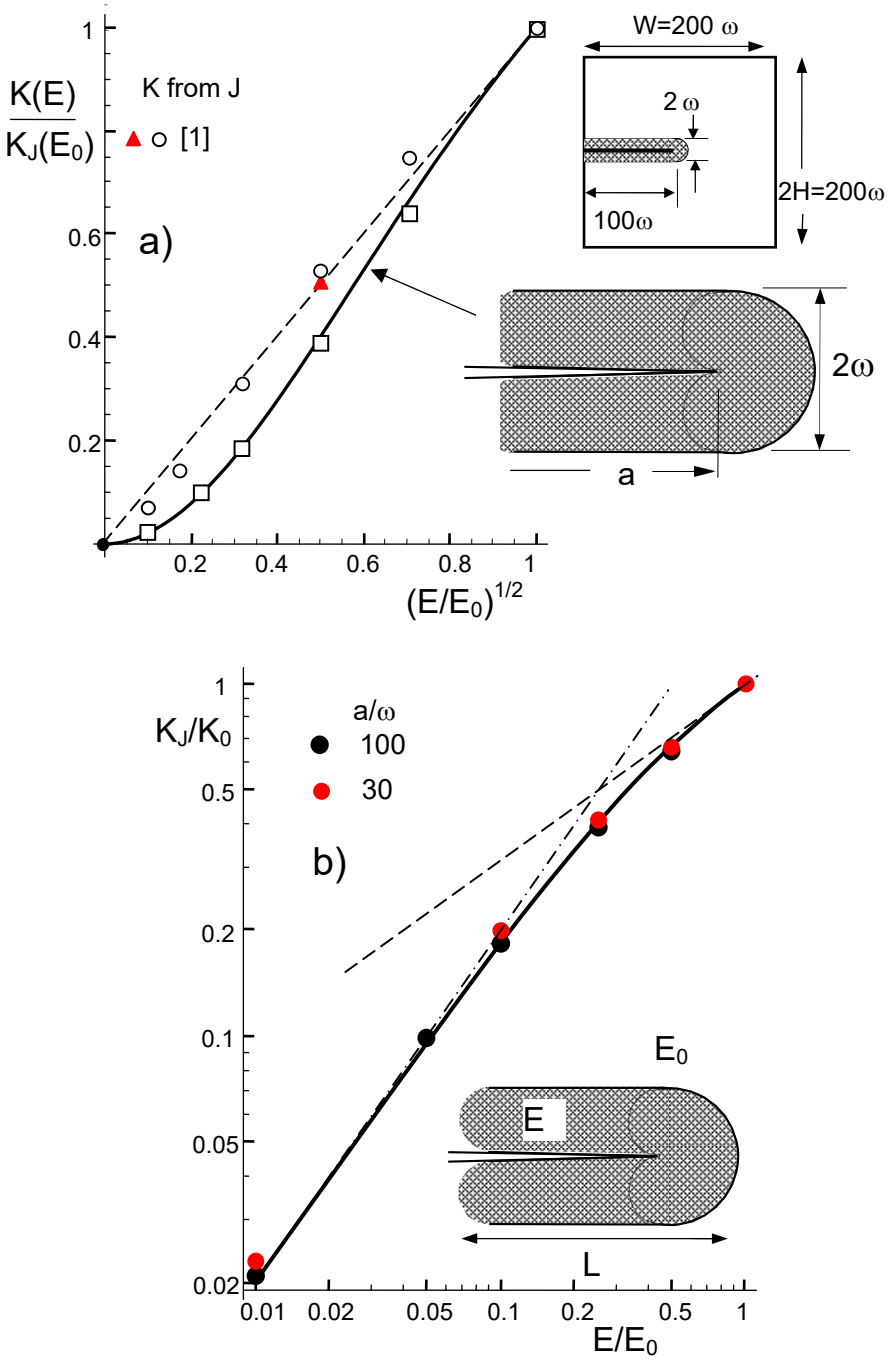

Fig. 4 a) Stress intensity factors from J-Integral, K_J (normalized on the value K_0 obtained for E=E_0) for embedded crack tips (squares) compared with the results of Fig. 2a (only K_J plotted by circles and triangle), solid curve: Approximation via eq.(4), b) Stress intensity factors from J-Integral, dashed line: asymptote with slope=1/2, dash-dotted line: asymptote with slope=1.

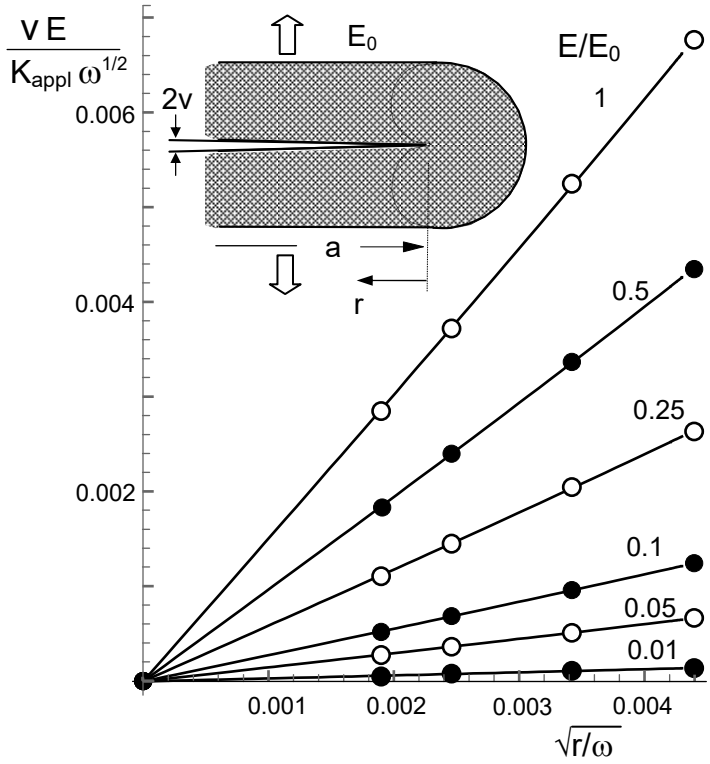

Fig.5 Crack-opening profiles close to the tip versus $(r/\omega)^{1/2}$ for a crack of a/ω=100.

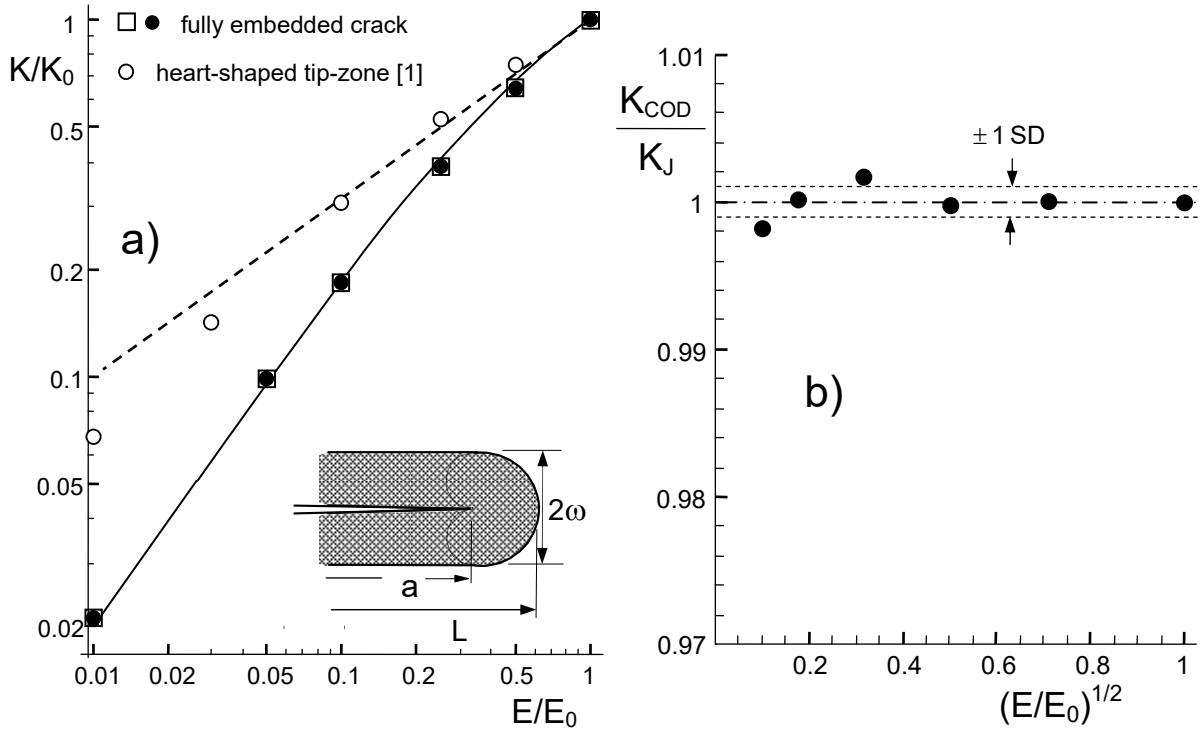

Fig. 6 a) K_J/K_0 vs. E/E_0 as squares, results from [1] as open circles, K_{COD} from Fig. 5 via eq.(5) as solid circles, b) ratio K_{COD}/K_J vs. $(E/E_0)^{1/2}$.

The stress intensity factors from eq. (5) are plotted in Fig. 6a as the solid circles together with the results from the J-Integral in Fig. 4a as the squares. In this representation no differences of the two *K*-values can be seen. Figure 6b shows the ratio of the two stress intensity factors. Note the significantly higher resolution of the ordinate.
The mean value and the standard deviation SD (in brackets) are

$$\frac{K_{COD}}{K_J} = 0.999987\,[0.001134]$$

Although in principle no theoretical facts can be proven by numerical calculations, this good agreement of the *K* factors speaks for the validity of K_J using different methods.

3. Derivation of J-Integral for slender notches by Merkle [3]

In a micro-structurally motivated approach, the crack tip region is considered as a slender notch with root radius ρ in the order of the average radius of the SiO_2 rings. For such a notch, Wiederhorn et al. [4] suggest a crack-tip radius of ρ = 0.5 nm. This description may be applied in the following considerations.
Merkle [3] showed that the relation (1) is exact in the case of a slender notch ending in a region of Young's modulus *E* different from the bulk material E_0.
In his analytical derivation he assumes a crack in an infinite body loaded by remote tension in *y*-direction resulting in the applied stress intensity factor K_{appl}. Our FE-computations were carried out on a finite rectangular plate (insets in Fig. 2a and Fig. 4a).

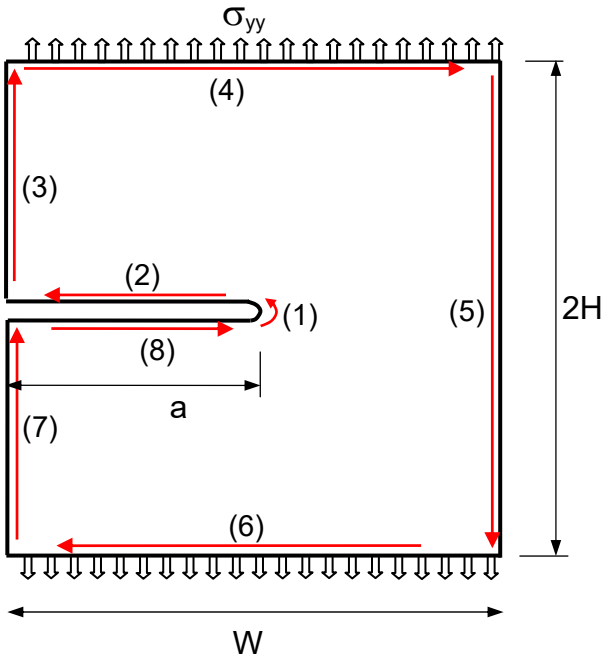

Fig. 7 Integration path for J-evaluation (red arrows)

The stress intensity factors were evaluated via the J-integral defined by

$$J = \int_{\Gamma} W\, dy - \mathbf{T}\frac{\partial u}{\partial x} ds \tag{6}$$

where W is the strain energy density, Γ the path around the crack tip, $\mathbf{T}$ the tractions on the path, u the displacement in y-direction, and ds a length increment of Γ.
For reasons of simplicity we used the usual path along the surfaces represented in Fig.°7 as the line segments (1)-(8). Along the contours (3), (5) and (7) no tractions act and on (4) and (6) constant tensile stresses are prescribed.
The J-integral along the surface segment (1) is

$$J_1 = \int_{\Gamma_1} W\, dy \tag{7}$$

In order to simplify the path-integration, the slender notch was approximated by a narrow elliptic notch with parabolic end shape (Fig. 8).
An arbitrary point on the red surface of Fig. 8c is described by the geometrical inter-relations

$$y = r\sin\varphi\,, \quad r = \frac{\rho}{1+\cos\varphi} \Rightarrow dy = \frac{\rho d\varphi}{1+\cos\varphi} \tag{8}$$

First it has to be noted that in the J-Integral only the modulus at the surface, E_s, enters and the variation with the distance from the surface doesn't play any role. In a subcritically grown crack the value E_s is constant along the whole notch surface.
Merkle [3] showed that the elastic strain energy along the crack surfaces (1, 2, 8) is

$$W = \frac{\sigma_t^2}{2E'} = \frac{K^2}{E'}\frac{\cos^2(\varphi/2)}{\pi r} \tag{9}$$

with the tangential stresses σ_t. From the geometrical relations of eq.(8) it follows after a simple mathematical manipulation

$$W = \frac{K^2}{E'}\frac{(1+\cos\varphi)^2}{2\pi\rho} \tag{10}$$

Consequently, the J-integral along path parts (1,2,8) reads

$$J_1 = \frac{K^2}{E'}\frac{1}{2\pi}\int_{-\pi}^{\pi}(1+\cos\varphi)d\varphi \Rightarrow J_1 = \frac{K^2}{E'} \tag{11}$$

This of course holds for large zones, $\omega>\rho$ to $\omega>>\rho$, for which $\varphi\rightarrow\pi$ can be sufficiently fulfilled. The J-integral along a closed path must disappear as shown by Rice [2]. Consequently, it must hold from the path parts (4) and (6), loaded by tensile tractions

$$J_{4,6} = \frac{K_{appl}^2}{E'} \tag{12}$$

with the applied stress intensity factor K_{appl}. Since the results (11) and (12) no longer depend on the notch radius, they should also apply to the sharp crack by taking $\rho \rightarrow 0$.

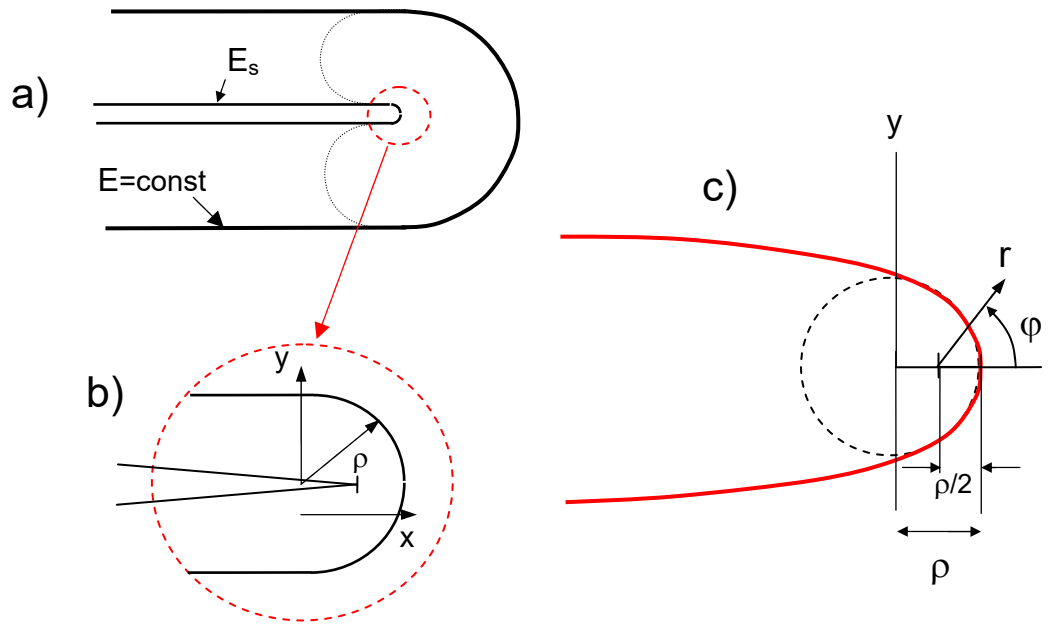

Fig. 8 a) Contour of constant hydrostatic stress at the tip of a subcritically grown crack, b) detail of a), c) crack surface approximated by an elliptical notch showing the same curvature radius ρ, schematic.

Final Remark:

From the FE results obtained in Report [1], and the theoretical solution by Merkle [3]

$$K = K_{appl}\sqrt{\frac{E}{E_0}}$$

it becomes clear that the FE-results for relative zone sizes $\omega/a > 0$ must deviate from the exact solution but may be also in rather good agreement with the theoretical results for finite ω/a.

Already here, it should be mentioned, that the derivation by Merkle [3] deals with the case of a zone of different Young's modulus ahead of a crack tip due to the finite notch root radius $\rho > 0$. The tip of the corresponding fictive crack is always in the distance $\rho/2$ from the notch root. Even when the radius ρ becomes smaller in the limit-case consideration, the geometry of Figs. 8b and 8c remains self-similar.

References

1 G. Rizzi, K.G. Schell, C. Bucharsky, T. Fett, FE-Study on heart-shaped crack-tip zones, **142**, 2020, ISSN: 2194-1629, Karlsruhe, KIT

2 Rice, J.R., A path independent integral and the approximate analysis of strain concentration by notches and cracks, Trans. ASME, J. Appl. Mech. (1986), 379-386.

3 J. G. Merkle, An application of the J-integral to an incremental analysis of blunt crack behavior, Mechanical Engineering. Publications, London, 1991, 319-332.

4 S.M. Wiederhorn, E.R. Fuller, Jr. and R. Thomson, "Micromechanisms of crack growth in ceramics and glasses in corrosive environments," Metal Science, **14**(1980), 450-8.

KIT Scientific Working Papers
ISSN 2194-1629

www.kit.edu